Fish and Shellfish Immunology 84 (2019) 138–147

Contents lists available at ScienceDirect

Fish and Shellfish Immunology

journal homepage: www.elsevier.com/locate/fsi

Full length article

Macropinocytosis-dependent endocytosis of Japanese flounder IgM$^+$ B cells and its regulation by CD22

Yi-qun Li[a,b,c], Li Sun[a,b,**], Jun Li[b,d,*]

[a] CAS Key Laboratory of Experimental Marine Biology, Institute of Oceanology, Center for Ocean Mega-Science, Chinese Academy of Sciences, Qingdao, China
[b] Laboratory for Marine Biology & Biotechnology and Laboratory for Marine Fisheries Sciences and Food Production Processes, Qingdao National Laboratory for Marine Science and Technology, Qingdao, 266071, China
[c] University of Chinese Academy of Sciences, Beijing, China
[d] School of Biological Sciences, Lake Superior State University, Sault Ste. Marie, MI, 49783, USA

ARTICLE INFO

Keywords:
Paralichthys olivaceus
IgM$^+$ B cells
Endocytosis
Macropinocytosis
CD22
B cell regulation

ABSTRACT

B cells in fish are proven to be endocytic and have a great contribution to innate immunity like phagocytosis. In this study, the endocytic capacity and the corresponding internalization pathways of IgM$^+$ B cells in Japanese flounder *(Paralichthys olivaceus)* were investigated. The results showed that IgM$^+$ B cells in peripheral blood leukocytes (PBL) and splenic leukocytes (SL) exhibited different abilities to ingest 0.5 μm and 1 μm latex beads through macropinocytosis-dependent endocytic pathway. Japanese flounder CD22 (PoCD22) co-stimulatory signals were identified to be essential for the innate immune responses in B cells. Most of IgM$^+$ B cells and some IgM$^-$ cells were demonstrated to be PoCD22 positive. When PoCD22 was blocked by antibody, the endocytic activities and reactive oxygen species (ROS) activities of SL IgM$^+$ B cells were significantly increased, while the endocytic and ROS activities of PBL IgM$^+$ B cells were significant decreased. These results collectively suggest that Japanese flounder IgM$^+$ B cells are able to employ macropinocytosis-dependent endocytic pathway, which is under the regulation of CD22.

1. Introduction

It is well known that B cells in teleost fish have endocytic capacity, and they can phagocytose particular antigens and induce phagolysosome formation and serial downstream degradative activities [1]. Endocytic B cells have so far been identified in many fish species, such as rainbow trout, zebrafish, lumpfish (*Cyclopterus lumpus* L.), half-smooth tongue sole (*Cynoglossus semilaevis*), Atlantic salmon (*Salmo salar* L.), Atlantic cod (*Gadus morhua* L.) and turbot (*Scophthalmus maximus*) [1–7]. So far, three types of immunoglobulins (IgM, IgT, and IgD) have been reported in teleost fish, and IgM, which consists of membrane IgM (B cell receptor, BCR) or soluble IgM, has been demonstrated as the most predominant isotype in teleost fish [8,9]. Membrane IgM$^+$ B cells are the majority B cells in teleost fish as have been demonstrated in salmon and rainbow trout [1,3].

Several endocytosis pathways, such as clathrin-dependent endocytosis, caveolin-dependent endocytosis, macropinocytosis and phagocytosis, have been reported to be involved in the process of particulate antigen internalization [10–13]. For example, human Raji B cells could ingest non-specific bacteria mainly through the pathway of macropinocytosis [14]. Similarly, macropinocytosis pathway was also involved in the internalization of large particles by turbot IgM$^+$ B cells [7]. However, clathrin- and caveolin-dependent pathways, rather than micropinocytosis, were used in IgM$^-$ cells to mediate the endocytosis of large particles [7]. Such specific pathway mediated endocytosis can be inhibited by related pharmacological compounds. Previous studies showed that clathrin-dependent endocytosis can be blocked with CPZ and dynasore; caveolin-dependent endocytosis can be inhibited by M-β-CD and nystatin; and macropinocytosis can be down-regulated by IPA-3 and NSC23766 [15]. Thus far, the endocytic pathways and related regulatory mechanisms involved in the particle internalizing process of phagocytic B cells in Japanese flounder *(Paralichthys olivaceus)* are not fully described yet.

B cell receptor (BCR) and B cell-associated receptors are essential for B cell activation through specific antigen recognization and signal transduction [16,17]. CD22, a B cell-associated receptor, can bind to alpha 2, 6-galactose-linked sialic acids and provide a co-stimulatory signal for activation of B cell. CD22 has been found to distribute

* Corresponding author. School of Biological Sciences, Lake Superior State University, 650 W. Easterday Ave. Sault Ste. Marie, MI, 49783, USA.
** Corresponding author. Institute of Oceanology, Chinese Academy of Sciences, 7 Nanhai Road, Qingdao, 266071, China.
E-mail addresses: lsun@qdio.ac.cn (L. Sun), jli@lssu.edu (J. Li).

https://doi.org/10.1016/j.fsi.2018.09.068
Received 24 June 2018; Received in revised form 2 September 2018; Accepted 24 September 2018
Available online 25 September 2018
1050-4648/ © 2018 Elsevier Ltd. All rights reserved.

throughout the body and play vital roles such as inhibition of BCR signaling via recruitment of SHP-1 phosphatase, as well as facilitation of adhesion between B cells and other type of cells [18]. In mammals, CD22 has been demonstrated as a negative regulator for antigen receptor signaling, and its onset of expression in mature B cells may serve to raise the threshold of antigen concentration required for B cell activation [19]. However, a positive signaling role for CD22 has also been observed for stimulating human B cell proliferation in the presence of antigen [20]. In our previous study, tongue sole CD22 was found to play an inhibitory role in peripheral blood leukocytes (PBL) activation [21], however, its potential effect on the activation of B cells remains to be investigated.

In the present study, we investigated the endocytic activity and pathway of IgM^+ B cells, as well as the regulating function of CD22 in B cell activation in Japanese flounder (*Paralichthys olivaceus*). Our results indicated that IgM^+ B cells, in both PBL and splenic leukocytes (SL), employed micropinocytosis-pathway to mediate the endocytosis of large particles in Japanese flounder, and CD22 showed different effects on the activation of IgM^+ B cells in PBL and SL.

2. Materials and methods

2.1. Fish

Japanese flounder (*Paralichthys olivaceus*), average 22 cm in length and 600 g in weight, were obtained from a commercial fish farm in Shandong Province, China and maintained at 19–20 °C in aerated seawater. Before experiment, fish were acclimatized to laboratory conditions for two weeks and confirmed to be absent of specific bacterial pathogens as previously described [21].

2.2. Leukocyte isolation

PBL preparation was performed based on previous report [22]. Blood was collected from the caudal vein of Japanese flounder after the fish were euthanized by being immersed in tricaine methanesulfonate solution (Sigma-Aldrich, St. Louis, USA) at the dose of 0.1 g/L in sterilized seawater. Blood was diluted immediately 1:4 with L-15 culture medium (Jinuo, Hangzhou, China) supplemented with 10 units/mL heparin (Solarbio, Beijing, China). Spleen was then collected and placed into a 50 mL test tube containing 30 mL of L-15 culture medium. The tissue was processed by being passed through a 100 μm nylon Falcon cell strainer (BD Falcon, Lexington, KY, USA). All cell suspensions were placed onto a 35/58% discontinuous Percoll (GE Healthcare) density gradients and centrifuged at 400 × *g* for 30 min. The PBL or SL from the interface layer were collected and washed twice with L-15 medium respectively (Gibco, Carlsbad, USA), and then re-suspended in L-15 culture medium containing 4% calf serum (Gibco, Carlsbad, USA), 100 U/mL penicillin (Solarbio, Beijing, China), 100 μg/mL streptomycin (Solarbio, Beijing, China), and 10 units/mL heparin.

2.3. Phagocytosis assay by flow cytometry

The phagocytic capability of Japanese flounder PBL and SL was evaluated as previously described [1]. Briefly, PBL or SL (1×10^6 cells/mL) were incubated with yellow green microsphere beads (Polysciences, Warrington, PA, USA, Fluoresbrite R Yellow Green, λ_{ex}, 445 nm; λ_{em}, 500 nm) of 0.5 μm or 1 μm in diameter at a cell/beads ratio of 1/10 for 4 h at 20 °C respectively. Non-ingested beads were removed by centrifuging (100 × *g* for 10 min at 4 °C) the cell suspension over a cushion of 3% BSA (Aikerbo, Qingdao, China) in PBS supplemented with 4.5% D-glucose (Sigma-Aldrich, St. Louis, USA). Then the phagocytic cells were resuspended in L-15 culture medium and incubated with 5 μg/mL mouse-anti-Japanese flounder IgM monoclonal antibody (mAb) (Aquatic Diagnostics Ltd, Stirling, Scotland) for 1 h at 20 °C, followed by staining with Phycoerythrin (PE)-conjugated goat anti-mouse IgG (Thermo Fisher Scientific, MA, USA) for 1 h at 20 °C. After washing, the phagocytosis of PBL or SL cells were determined by a FACScan flow cytometer (BD Biosciences, USA), and following data analysis by FlowJo.

2.4. Effect of endocytosis inhibitors on leukocyte uptake of microspheres

Microsphere uptake was performed as reported previously [7]. PBL or SL (1×10^6 cells/mL) were pretreated with various inhibitors, i.e., 20 μM chlorpromazine (CPZ) (Selleck, USA), 15 μM dynasore (Selleck, USA), 1 mM methy-β-clodextrin (M-β-CD) (Sigma-Aldrich, St. Louis, USA), 100 μM nystatin (Selleck, USA), 40 μM IPA-3 (Selleck, USA), 100 μM NSC23766 (Selleck, USA), in L-15 medium for 2 h at 20 °C, respectively. The pre-treated PBL or SL were then incubated with microspheres (size 0.5 μm or 1 μm) for 4 h or 2 h at 20 °C. After being washed three times with PBS, the PBL or SL were fixed with 4% paraformaldehyde. After staining with anti-Japanese flounder IgM mAb and PE-conjugated second antibody as described above, the cells were then subjected to FACScan analysis.

2.5. Sequence analysis

The mRNA sequence (GenBank accession no. XM_020091019.1) and amino acid sequence (GenBank accession no. XP_008321463.1) of *PoCD22* was analyzed using the BLAST program at the National Center for Biotechnology Information (NCBI, http://blast.ncbi.nlm.nih.gov/Blast.cgi). Domain search was performed with the conserved domain search program of NCBI. The theoretical molecular mass and isoelectric point were predicted by using online analysis tool ExPASy (https://web.expasy.org/compute_pi/). Sequence alignment was created with DNAMAN. Phylogenetic analysis was performed with the neighbor-joining algorithm of MEGA 6.0.

2.6. Purification of recombinant protein and preparation of antibody

To construct pETPoCD22, which expresses the extracellular region of PoCD22 (residues 52 to 899), the coding sequence of this region was amplified by PCR with primers F1 (5′-GATATCGGAGATTGGAGCGTG ACCTTT-3′, underlined sequence, *Eco*RV site) and R1 (5′-GATATCCGT CTGGCTGCCGTGG-3′, underlined sequence, *Eco*RV site) and cDNA of spleen was used as the template; the PCR products were ligated with the TA cloning vector T-Simple (TransGen Biotech, Beijing, China), and the recombinant plasmid was digested with *Eco*RV to retrieve the PoCD22-containing fragment, which was inserted into pET32a (Novagen, San Diego, USA) at the *Eco*RV site. rPoCD22 as a fusion protein with the TRX derived from pET32a was purified as described previously [23]. Briefly, *Escherichia coli* BL21 (DE3) (TransGen Biotech, Beijing, China) was transformed separately with pETPoCD22 and pET32a (Novagen, San Diego, USA), which expressing TRX; the transformants were cultured in LB medium at 37 °C to mid-logarithmic phase, and isopropyl-β-D-thiogalactopyranoside (IPTG) was added to the culture to a final concentration of 0.1 mM. After growing at 16 °C for an additional 16 h, the cells were harvested by centrifugation, and His-tagged recombinant PoCD22 (rPoCD22) and rTRX was purified using NiNTA Agarose (QIAGEN, Valencia, USA) following the manufacturer's instruction. The rPoCD22 and rTRX proteins were dialyzed against 1 × PBS (pH 8.0) and then concentrated with PEG20000 (Sigma -Aldrich, St. Louis, USA). The concentrated protein was analyzed in 12% sodium dodecyl sulfate-polyacrylamide gel electrophoresis (SDS-PAGE) and stained with Coomassie Brilliant Blue R-250 (Fig. S2). The concentration of the purified protein was determined using the Bradford method with bovine serum albumin (BSA) as a standard. Rat anti-rPoCD22 and anti-rTRX antiserum were generated as reported previously [24]. The specificity of the antiserum was confirmed by Western blot analysis as reported previously [25].

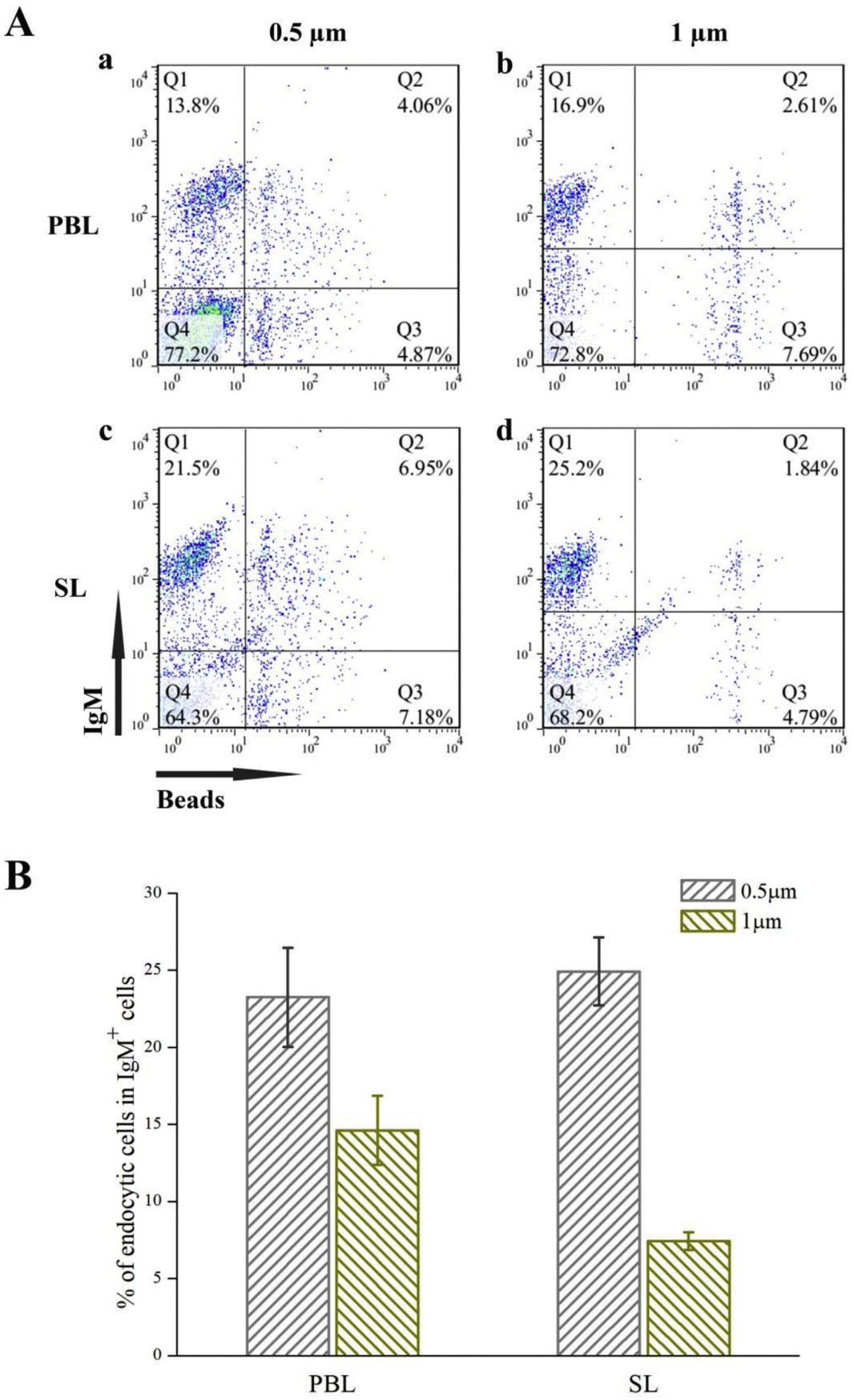

Fig. 1. Flow cytometry analysis. (A) Peripheral blood leukocytes (PBL) and splenic leukocytes (SL) were incubated with 0.5 μm or 1 μm beads and treated with IgM specific antibodies. (B) Uptake rate of 0.5 μm and 1 μm beads by IgM^+ cells in PBL and SL. Data are representatives of three independent experiments.

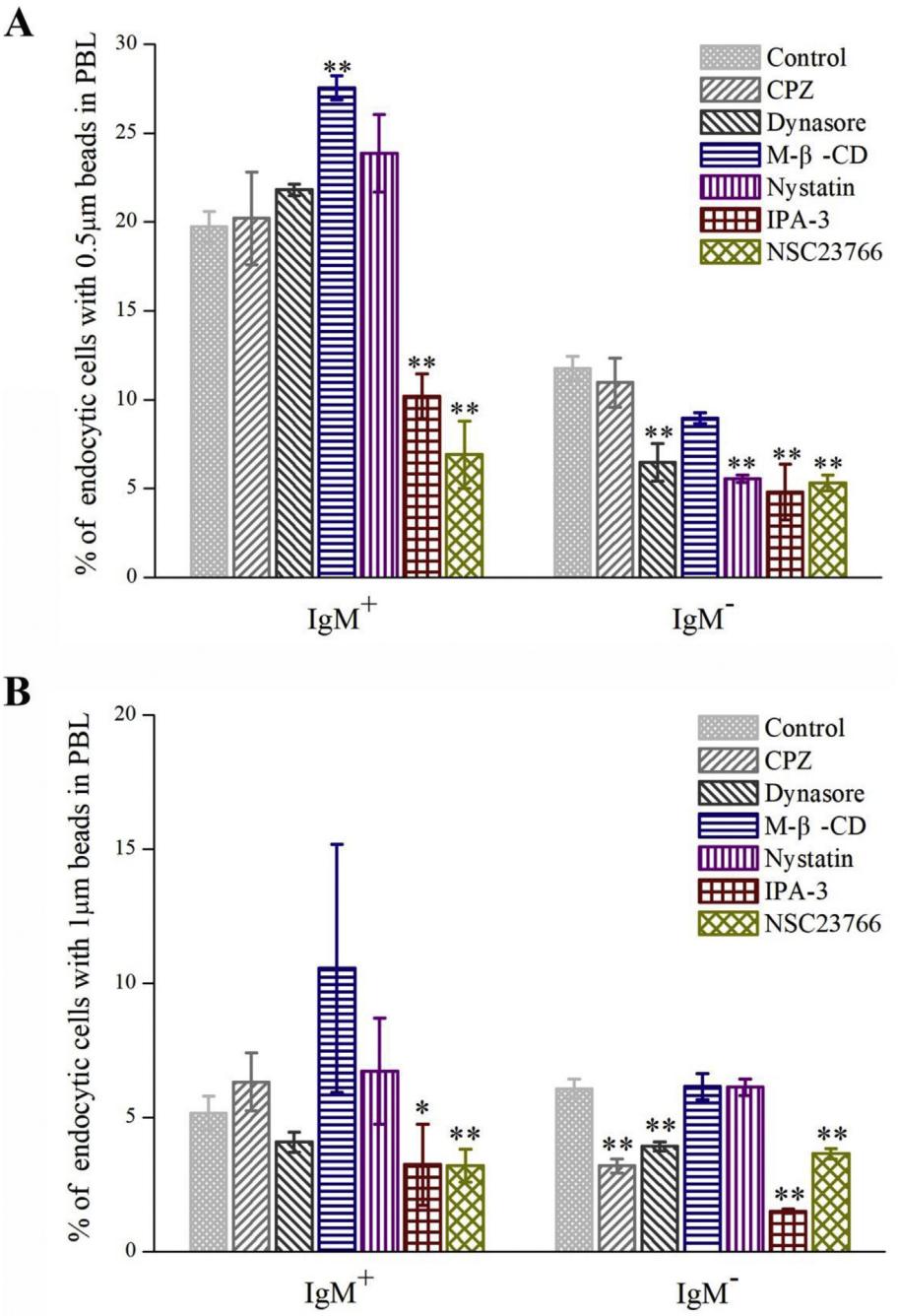

Fig. 2. Effect of endocytic pathway inhibitors on the uptake of 0.5 μm and 1 μm beads by IgM^+ and IgM^- cells in peripheral blood leukocytes (PBL). A. Endocytic rate of IgM^+ cells and IgM^- cells for 0.5 μm beads in the presence of inhibitors (CPZ, dynasore, M-β-CD, nystatin, IPA-3, and NSC23766). B. Endocytic rate of IgM^+ cells and IgM^- cells for 1 μm beads in the presence of inhibitors. Data are obtained from three independent experiments. *, $P < 0.05$; **, $P < 0.01$.

2.7. Immunofluorescence and flow cytometry

Five hundred microliters of PBL or SL suspension (10^5 cells/mL) was added to confocal dishes (35 mm) and incubated for 2 h at 20 °C. The cells were then fixed with 4% paraformaldehyde (Solarbio, Beijing, China) and blocked with 3% BSA for 30 min. After treating with 5 μg/mL mouse-anti-Japanese flounder IgM mAb and Alexa Fluor 594 labeled-goat anti-mouse IgG (Abcam, Shanghai) for 1 h at 20 °C, the cells were washed three times with PBS and then treated with anti-rCsCD22 antiserum (1:1000 dilution in 3% BSA in PBS) and Alexa Fluor 488 labeled-goat anti-rat IgG (Abcam, Shanghai). The cells were stained with 4', 6-diamidino-2-phenylindole (DAPI, 10 μg/mL) (Solarbio, Beijing, China) for 10 min at 20 °C and then subjected to confocal microscope examination (Zesis LSM710, Germany).

For flow cytometric analysis, PBL and SL were incubated with mouse anti-Japanese flounder IgM mAb and PE-conjugated goat anti-mouse IgG as described above. Then the cells were stained with rat anti-rPoCD22 antiserum (1:1000 dilution in 3% BSA in PBS) at 37 °C for 1 h. After three washes with PBS, the cells were stained with FITC-labeled goat-*anti*-rat secondary antibody at 37 °C for 1 h and then were subjected to flow cytometric analysis.

2.8. Effect of rPoCD22 antiserum on phagocytic activity

PBL and SL were incubated with rat anti-rPoCD22 antiserum (1:500 dilution), rat anti-rTRX antiserum (1:500 dilution) or PBS at 22 °C for

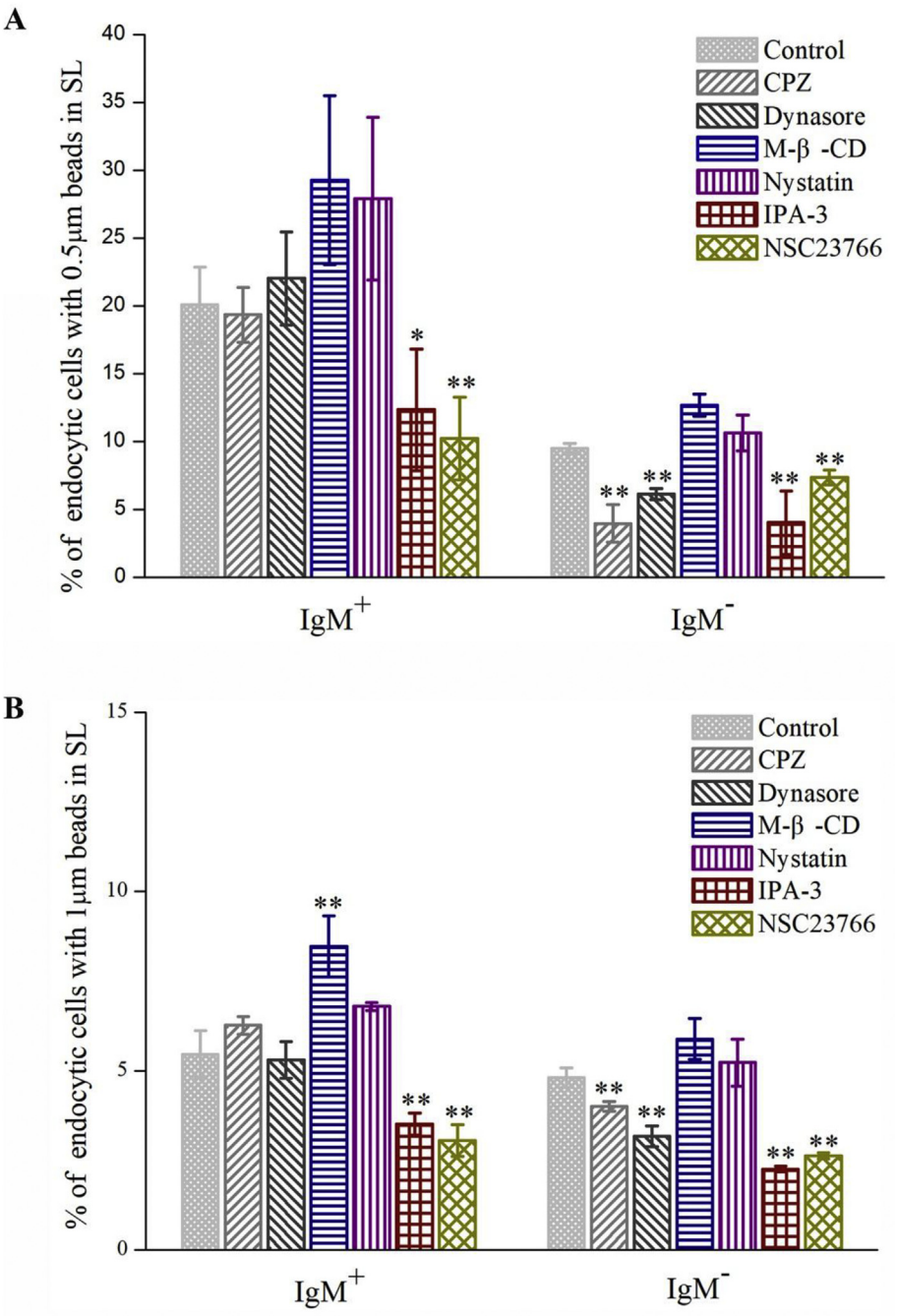

Fig. 3. Effect of endocytic pathway inhibitors on the uptake of 0.5 μm and 1 μm beads by IgM^+ cells and IgM^- cells in SL. A. Endocytic rates of IgM^+ cells and IgM^- cells for 0.5 μm beads in the presence of inhibitors (CPZ, dynasore, M-β-CD, nystatin, IPA-3, and NSC23766). B. Endocytic rates of IgM^+ cells and IgM^- cells for 1 μm beads in the presence of inhibitors. Data are obtained from three independent experiments. *, $P < 0.05$; **, $P < 0.01$.

2 h, respectively. The cells were washed and resuspended in L-15 medium to 1×10^7 cells/ml. *Vibrio harveyi* was cultured in LB medium to an OD_{600} of 0.8, and labelled with FITC (100 mg/mL FITC dissolved in dimethylsulfoxide). PBL and SL (1×10^7 cells/mL) were then incubated with 1×10^8 CFU/mL FITC-labeled *V. harveyi* in the dark at 28 °C for 2 h. The cells were collected by centrifugation, washed five times in PBS, and resuspended in L-15 medium to 1×10^6 cells/mL. After fixation with 4% paraformaldehyde, the cells were stained firstly with mouse anti-Japanese flounder IgM mAb and then with PE-conjugated second antibody as described above, and then subjected to FACScan analysis.

2.9. Cell sorting and effect of rPoCD22 antiserum on cellular ROS activity

Japanese flounder PBL and SL were separately incubated with mouse anti-Japanese flounder IgM mAb and PE-conjugated goat anti-mouse IgG as above. Then IgM^+ B cells were sorted out by using FACScan flow cytometer (BD Biosciences) sorting system and collected in tubes containing L-15 medium, 4% calf serum and 100 U/mL penicillin (Solarbio, Beijing, China), 100 μg/mL streptomycin.

The ROS levels in sorted IgM^+ B cells were measured with a 2,7-dichlorofluorescin diacetate (DCFH-DA) cellular ROS assay kit (Beyotime, Beijing, China) according to the manufacture's instruction. Briefly, sorted IgM^+ B cells (10^6 cells/mL) were incubated with rat anti-rPoCD22 antiserum (1:500 dilution), rat anti-rTRX antiserum (1:500

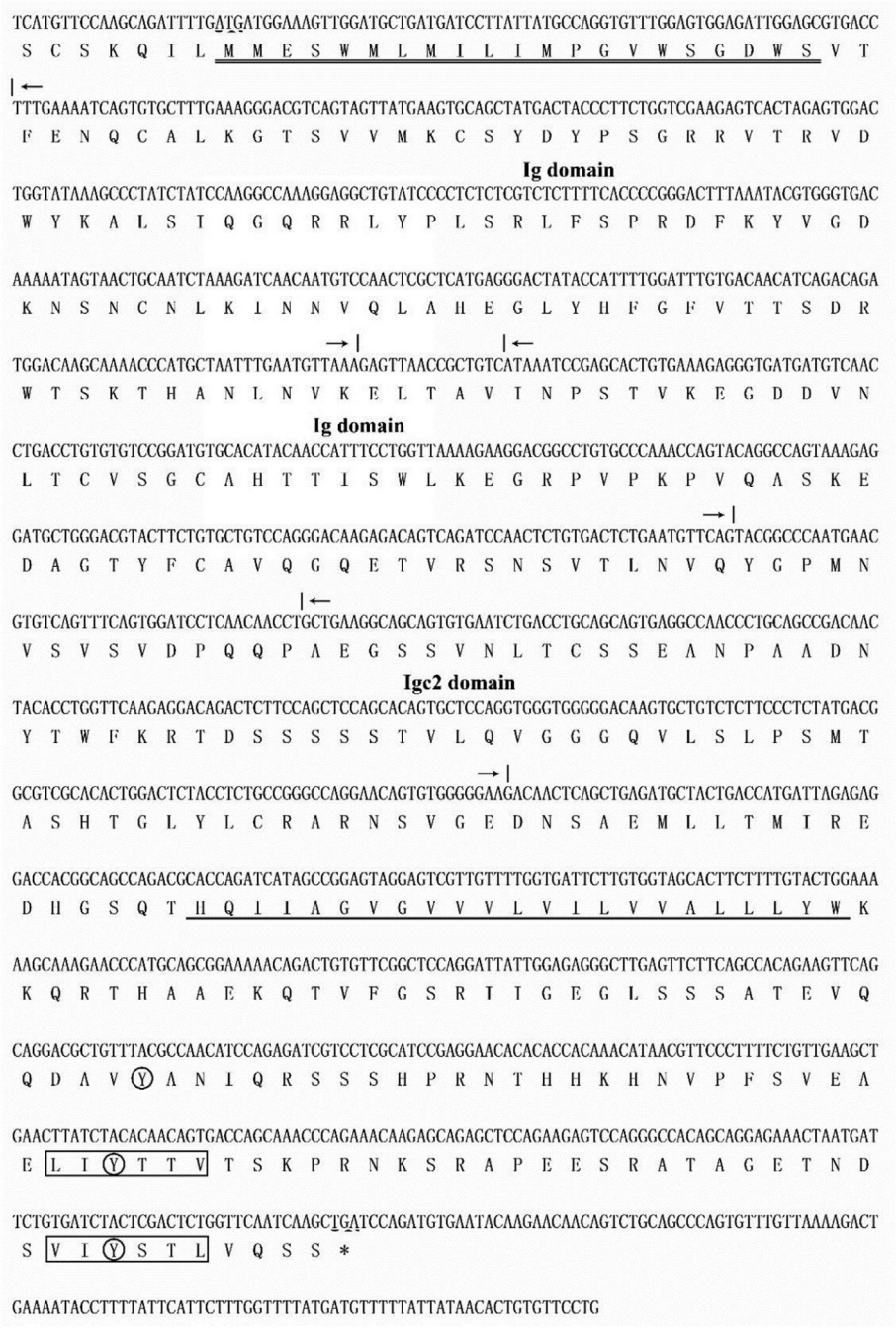

Fig. 4. cDNA and amino acid sequences of PoCD22. The start and stop codons are underlined with dotted line. Signal peptides and transmembrane hydrophobic regions are underlined with double and single line, respectively. The asterisk indicates peptide ending. The Immunoglobulin domain (Ig domain) and Immunoglobulin C2 type domain (Igc2 domain) are indicated by arrows; the immunoreceptor tyrosine-based inhibitory motifs (ITIMs) and conserved tyrosine residues are indicated by black box and circles, respectively.

dilution) or PBS (control) at 22 °C for 2 h, followed by incubation with 1×10^7 CFU/mL *V. harveyi* in the dark at 22 °C for 2 h. After incubation, cells were stained with DCFH-DA for 1 h at 17 °C in the dark. The fluorescence intensity of the cells was analyzed by FACScan flow cytometer. Relative ROS activity was calculated as percentage of the value for antiserum incubation group/control group.

2.10. Statistical analysis

All experiments were performed at least three times, and statistical analyses were carried out with SPSS 17.0 software (SPSS Inc., Chicago, IL, USA). Data were analyzed with analysis of variance (ANOVA), and statistical significance was defined as $P < 0.05$.

3. Results

3.1. Endocytic efficiency of Japanese flounder IgM$^+$ B cells

In Japanese flounder, approximately 13–18% of PBL and 24–27% of SL were IgM$^+$ cells. After incubation with fluorescent beads of different sizes, IgM$^+$ B cells were able to ingest the beads and the endocytic efficiencies were size-dependent (Fig. 1). In PBL, 23.24 ± 3.20% of IgM$^+$ B cells ingested 0.5 μm beads, and 14.62 ± 2.25% of IgM$^+$ B cells ingested 1 μm beads; in SL, 24.92 ± 2.20% of IgM$^+$ B cells

ingested 0.5 μm beads, and 7.43 ± 0.57% of IgM$^+$ B cells ingested 1 μm beads (Fig. 1B).

3.2. Effects of endocytic inhibitors

The endocytic pathways are mediated by various mechanisms and can be blocked with specific inhibitors. As shown by FACS analysis, the endocytic rate of PBL IgM$^+$ B cells for 0.5 μm beads decreased significantly ($P < 0.01$) in the presence of IPA-3 and NSC23766, the inhibitors of macropinocytosis, but not in the presence of CPZ, dynasore, M-β-CD, or nystatin, the inhibitors of clathrin and calveolin (Fig. 2A). Whereas, the uptake activity of PBL IgM$^-$ cells was significantly ($P < 0.01$) reduced in the presence of dynasore, M-β-CD, nystatin, IPA-3 and NSC23766, but not affected in the presence of CPZ (Fig. 2A). However, for 1 μm beads, the endocytic rate of PBL IgM$^+$ B cells was significantly ($P < 0.05$) reduced in the presence of IPA-3, NSC23766, but not in the presence of CPZ, dynasore, M-β-CD, or nystatin (Fig. 2B). The uptake ability of PBL IgM$^-$ cells was significantly ($P < 0.01$) reduced in the presence of CPZ, dynasore, IPA-3 and NSC23766, but not in the presence of M-β-CD or nystatin (Fig. 2B).

Similarly, the endocytic rate of SL IgM$^+$ B cells for 0.5 μm beads decreased significantly ($P < 0.05$) in the presence of IPA-3 and NSC23766, but not in the presence of CPZ, dynasore, M-β-CD, or nystatin (Fig. 3A). The uptake activity of SL IgM$^-$ cells for 0.5 μm beads was significantly ($P < 0.05$) reduced in the presence of CPZ, dynasore, IPA-3 and NSC23766, but was not affected in the presence of M-β-CD and nystatin (Fig. 3A). The endocytic rate of SL IgM$^+$ cells for 1 μm beads was significantly ($P < 0.01$) reduced in the presence of IPA-3, NSC23766, but not in the presence of CPZ, dynasore, M-β-CD, or nystatin (Fig. 3A). The uptake of 1 μm beads by SL IgM$^-$ cells was significantly ($P < 0.01$) reduced in the presence of CPZ, dynasore, IPA-3 and NSC23766, but not affected in the presence of M-β-CD or nystatin (Fig. 3B).

3.3. Sequence features of PoCD22

PoCD22 is composed of 424 amino acid residues with a calculated molecular mass of 46.62 kDa. Similar to mammalian CD22, PoCD22 contains two Ig domains (residues 24–125 and 131–198) and one Ig C2 (Igc2) type domain (residues 214–279). PoCD22 was predicted to be a transmembrane protein with a signal peptide (residues 1–17), a large N-terminal extracellular region (residues 1–299), a transmembrane region (residues 300–322), and an intracellular region (residues 323–424) (Fig. 4). Three tyrosines are present in the cytoplasmic tail, two of which being located in the conserved immunoreceptor tyrosine-based inhibitory motifs (ITIMs) (Fig. 4). Phylogenetic analysis showed that PoCD209 and the CD22 of *Synoglossus semilaevis* formed a cluster, which was separated from the groups formed by the CD22 of other teleost and mammals (Fig. S2).

3.4. Distribution of PoCD22 protein in PBL and SL

FACS analysis detected PoCD22 protein expression in IgM$^+$ and IgM$^-$ cells in Japanese flounder PBL and SL (Fig. 5A). Approximately 47% of PBL and 46% of SL were CD22 positive. In PBL, 76.31 ± 4.43% IgM$^+$ B cells were CD22 positive, whereas only 43.35 ± 7.90% of IgM$^-$ cells were CD22 positive; in SL, 78.72 ± 4.67% of IgM$^+$ cells were CD22 positive, and 36.93 ± 3.31% of IgM$^-$ cells were CD22 positive (Fig. 5A).

After staining with rat anti-rPoCD22 antiserum, the localization of CD22 can be observed under the immunofluorescence microscopy on the surface of nearly all the IgM$^+$ cells and part of IgM$^-$ cells from both PBL and SL (Fig. 5B).

3.5. Effect of anti-rPoCD22 antiserum on the endocytic activity of PBL and SL against infecting bacteria

Comparison between PBL infected with *V. harveyi* in the presence and absence of anti-rPoCD22 antiserum showed that the endocytic activity of PBL IgM$^+$ B cells for the bacterial cells was significantly ($P < 0.01$) decreased in the presence of anti-rPoCD22 antiserum, while the endocytic activity of PBL IgM$^-$ cells was significantly ($P < 0.01$) increased in the presence of anti-rPoCD22 antiserum (Fig. 6A and C). In contrast, the endocytic activity of *V. harveyi*-infected SL IgM$^+$ cells was significantly ($P < 0.05$) increased in the presence of anti-rPoCD22 antiserum, while the endocytic activity of *V. harveyi*-infected SL IgM$^-$ cells showed no significant change in the presence of anti-rPoCD22 antiserum (Fig. 6B and D).

3.6. Effects of anti-rPoCD22 antiserum on the ROS activity of PBL and SL during bacterial infection

To examine the ROS activities in PBL and SL during *V. harveyi* infection in the presence and absence of anti-rPoCD22 antiserum, FACS analysis was performed, which showed that the ROS activities were significantly ($P < 0.05$) decreased in PBL IgM$^+$ cells treated with anti-rPoCD22 antiserum in comparison to that of the PBL IgM$^+$ cells treated with anti-rTRX antiserum or PBS, while the ROS activities of PBL IgM$^-$ cells exhibited no significant change in the presence of anti-rPoCD22 antiserum (Fig. 7A). In SL, the ROS activities were significantly ($P < 0.01$) increased in IgM$^+$ cells in the presence of anti-rPoCD22 antiserum compared to control groups treated by anti-rTRX antiserum or PBS, whereas the ROS activities in SL IgM$^-$ cells were significantly ($P < 0.01$) decreased (Fig. 7B).

4. Discussion

Endocytic capacities of fish B cells have been observed in rainbow trout, Atlantic salmon, Atlantic cod, lumpfish, half-smooth tongue sole and turbot [1–3,5,7]. Similarly, in the present study, flow cytometry analysis revealed that IgM$^+$ B cells of Japanese flounder exhibited apparent capacity to uptake latex beads. The percentage of IgM$^+$ B cells and the endocytic activity for 0.5 μm in PBL and SL was similar, however, the endocytic activity of IgM$^+$ B cells for 1 μm in SL was lower in comparison to PBL IgM$^+$ B cells. For both PBL IgM$^+$ B cells and SL IgM$^+$ B cells, the endocytic efficiency dropped with the increasing of the size of the beads. These results indicated that IgM$^+$ B cells in PBL and SL showed different endocytic efficiency for different size particles, which suggest that PBL IgM$^+$ B cells and SL IgM$^+$ B cells might play different roles when they interact with different foreign particles. It is well known that spleen is the place for B cell differentiation and maturation, while peripheral blood contains effector lymphocytes. Our current observation about the endocytic difference of IgM$^+$ B cells in PBL and SL properly exhibited the immune difference between these tissues. Therefore, the effects of differentiation and maturation status of B cells on the endocytic activity and the related immune functions need to be further investigated.

It is well known that matured mammalian B cells could bind specific antigen through a unique and restricted BCR and internalize ligand-receptor complexes via a clathrin-dependent pathway [26,27]. However, Raji B cells (derived from Burkitt lymphoma) engulfed non-specific bacteria through micropinocytosis [14]. Our previous study demonstrated that the internalization of large particles by turbot PBL IgM$^+$ B cells relies on micropinocytosis-dependent pathway and can be inhibited by macropinocytic inhibitors [14]. In the present study, a number of pharmacological inhibitors related to clathrin-mediated endocytosis, caveolin-mediated endocytosis and macropinocytosis were investigated. Our results showed that the uptake of 0.5 μm and 1 μm beads by PBL and SL IgM$^+$ B cells were significantly decreased in the presence of IPA-3 and NSC23766 (macropinocytosis inhibitors).

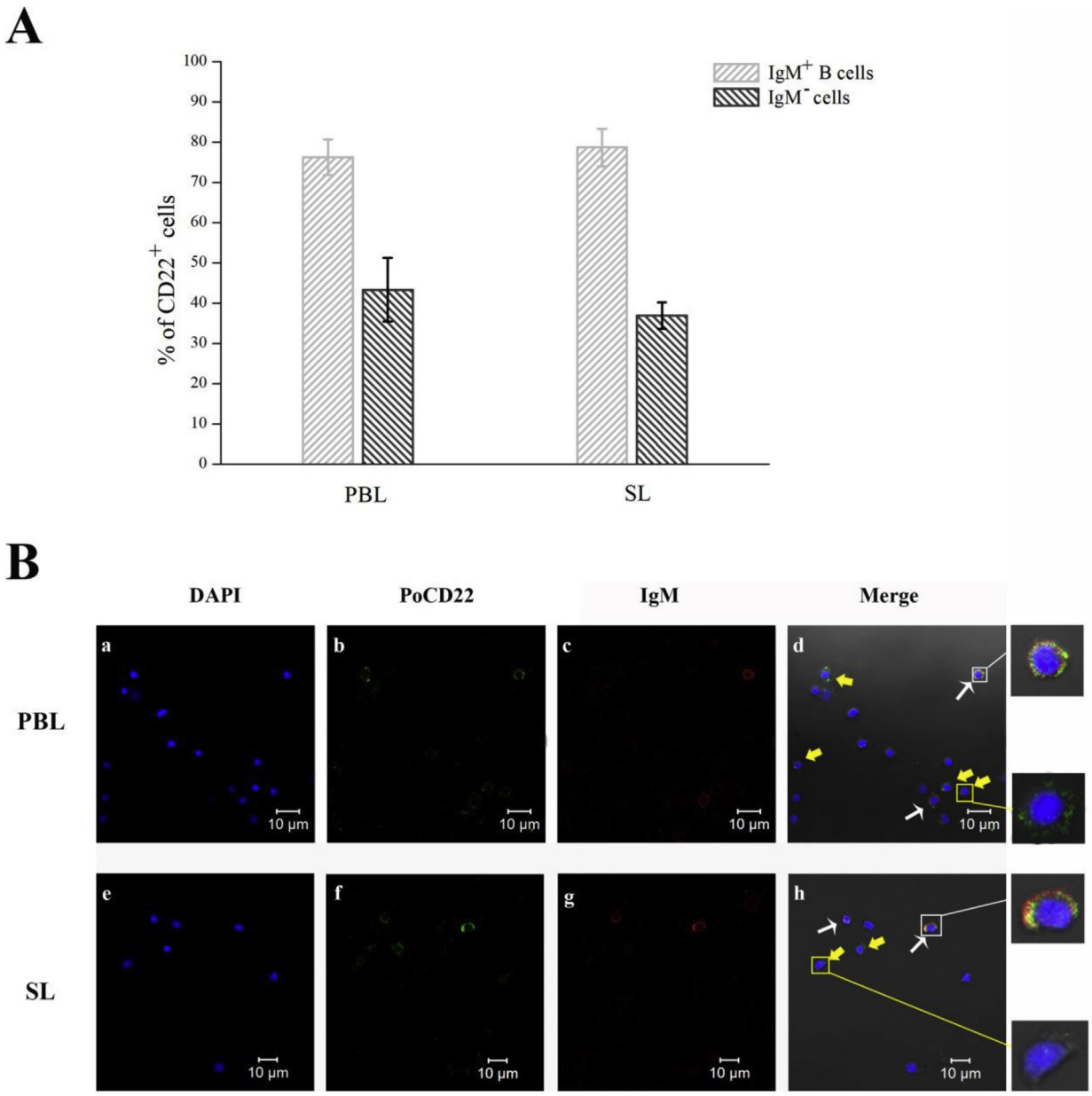

Fig. 5. PoCD22 protein expression in IgM$^+$ cells and IgM$^-$ cells. A. FACS analysis of the percentage of PoCD22$^+$ cells in IgM$^+$ B cells and IgM$^-$ cells from peripheral blood leukocytes (PBL) or spleen leukocytes (SL). PBL and SL were treated with anti-rPoCD22 antibody and subjected to flow cytometry. B. Confocal microscopy of PoCD22$^+$ cells in IgM$^+$ B cells and IgM$^-$ cells from PBL and SL. The cells were stained with DAPI and subjected to confocal microscopy. d, a merged image of a, b and c; h, a merged image of e, f and g. White arrows indicate IgM$^+$CD22$^+$ cells. Yellow arrows indicate IgM$^-$CD22$^+$ cells. Magnified views of the box regions of Fig. 5B d and Fig. 5B h are shown. Scale bar, 10 μm. Data are obtained from three independent experiments. (For interpretation of the references to colour in this figure legend, the reader is referred to the Web version of this article.)

However, for PBL IgM$^-$ cells, the uptake activity for 0.5 μm beads was significantly reduced in the presence of dynasore, M-β-CD, nystatin, IPA-3 and NSC23766, and the uptake activity for 1 μm beads was significantly reduced in the presence of CPZ, dynasore, IPA-3 and NSC23766. For SL IgM$^-$ cells, the uptake activities for both 0.5 μm beads and 1 μm beads were significantly reduced in the presence of CPZ, dynasore, IPA-3 and NSC23766. These observations indicated that micropinocytosis-dependent pathway was involved in the internalization of large particles by IgM$^+$ B cells derived from both PBL and SL of Japanese flounder.

In mammalian CD22, ITIM is one of the key motifs that functions for recruiting the potent phosphotyrosine and phosphoinositide phosphatases SHP-1 and SHIP [28–31]. Five Ig domains has been described in CD22 and three of the six tyrosine residues in cytoplasmic region are identified within ITIMs [32,33]. In our study, we found that the deduced amino acid sequence of PoCD22 contains two Ig domains and one Igc2 domain, which is consistent with the observations in other fish and mammalian CD22. However, in the cytoplasmic region of PoCD22, only three conserved tyrosine residues were detected, and two of them was found within ITIMs. These structural characteristics indicate that PoCD22 is a member of the CD22 family but differs distinctly from mammalian CD22.

Mammalian CD22 is a B cell-specific costimulatary molecule and widely distributed on the surface of mature B cells [30]. In fish, our previous study showed that tongue sole CD22 was localized on the surface of a small proportion of PBL assumed morphologically to be lymphocytes [21]. In the present study, we found that a majority of Japanese flounder IgM$^+$ B cells were PoCD22 positive, and some IgM$^-$

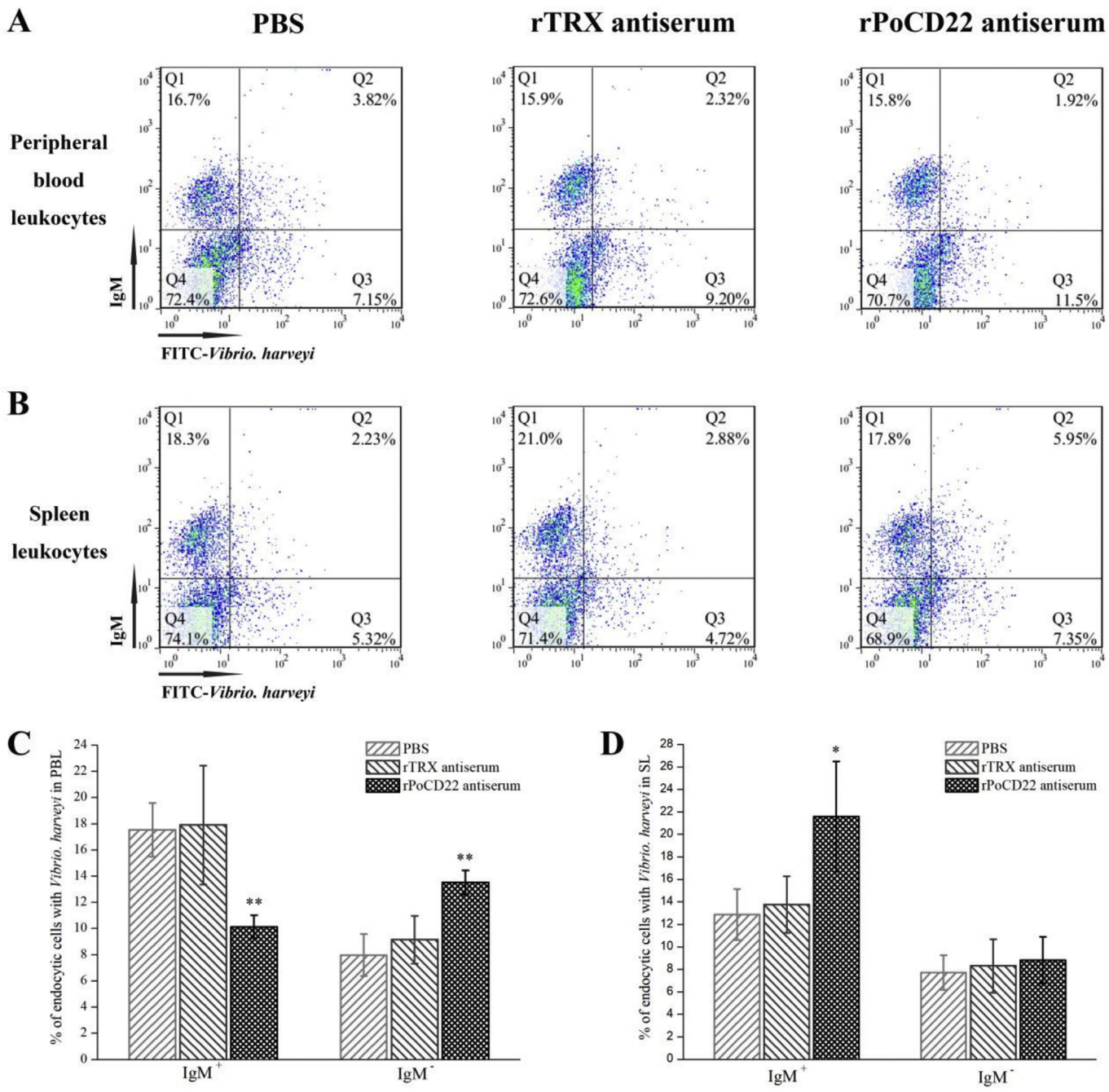

Fig. 6. Effect of anti-rPoCD22 antiserum on the endocytic activities of IgM^+ and IgM^- cells against infecting bacteria. A. FACS analysis of peripheral blood leukocytes (PBL) infected with *Vibrio harveyi* in the presence of PBS, anti-rTRX antiserum or anti-rPoCD22 antiserum. B. FACS analysis of splenic leukocytes (SL) infected with *V. harveyi* in the presence of PBS, anti-rTRX antiserum or anti-rPoCD22 antiserum. C. Endocytic rates of PBL IgM^+ cells and IgM^- cells for *V. harveyi* in the presence of PBS (control), anti-rTRX antiserum or anti-rPoCD22 antiserum. D. Endocytic rates of SL IgM^+ cells and IgM^- cells for *V. harveyi* in the presence of PBS (control), anti-rTRX antiserum or anti-rPoCD22 antiserum. Data are representatives of three independent experiments. *, $P < 0.05$; **, $P < 0.01$.

cells also expressed PoCD22 protein, suggesting that different subsets of B cells may exist in Japanese flounder, which will be investigated in future studies.

In mammals, CD22 is known to play an essential inhibitory role in B cell survival and signal transduction, and prevents overactivation of immune responses [29,30]. Nevertheless, positive regulation of CD22 has also been observed in human B cells [20]. In fish, tongue sole CD22 was reported to exhibit an inhibitory effect on the phagocytosis of PBL [21]. However, the role of CD22 in fish B cell activation remains unclear. In the present study, we found that the endocytic activity of PBL IgM^+ B cells against *V. harveyi* was significantly reduced in the presence of anti-rPoCD22 antibody, whereas the endocytic SL IgM^+ B cells was significantly increased in the presence of anti-rPoCD22 antibody; similar alterations in the ROS activities of PBL IgM^+ B cells and SL IgM^+ B cells by anti-rPoCD22 antibody were also observed. The results indicate that PoCD22 likely exerts different roles in PBL and SL IgM^+ B cell activity, which suggests that IgM^+ B cells in fish may have different missions during microbial infection.

In conclusion, we demonstrated for the first time that the particle uptake ability of Japanese flounder IgM^+ B cells varies in PBL and SL, but PBL IgM^+ B cells and SL IgM^+ B cells share the same endocytic pathway, macropinocytosis. The costimulatory molecule CD22 is

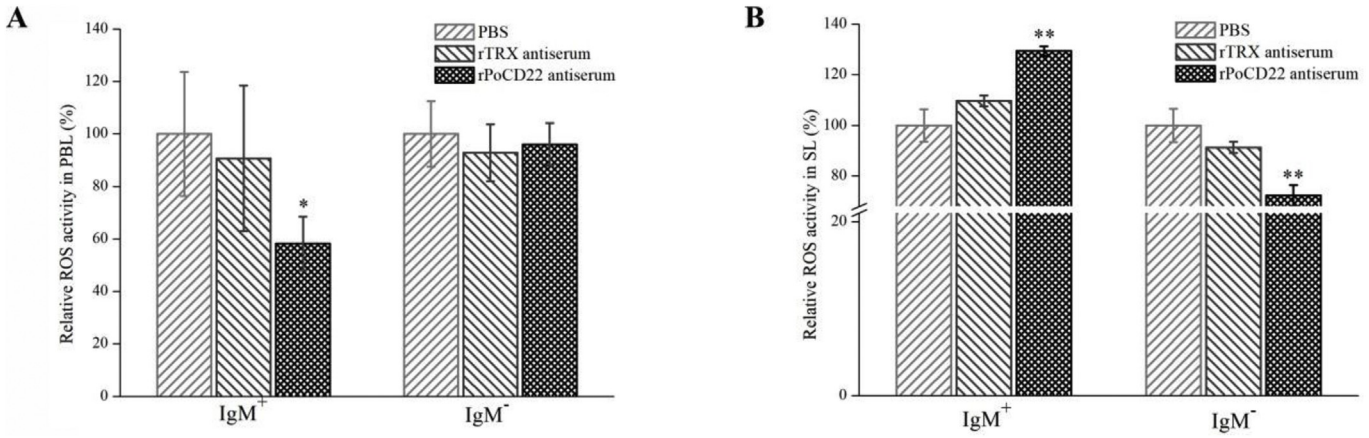

Fig. 7. Effects of anti-rPoCD22 antiserum on ROS activities of the IgM^+ and IgM^- cells of Japanese flounder peripheral blood leukocytes (PBL) and splenic leukocytes (SL). A. IgM^+ and IgM^- cells were sorted by FACS from PBL and incubated with PBS (control), anti-TRX antiserum or anti-rPoCD22 antiserum for 1 h. Then the cells were incubated with *Vibrio harveyi* for 1 h and stained with 2,7-dichlorofluorescin diacetate for 30 min. The fluorescence intensity of the cells was read using flow cytometry and the relative ROS activity was calculated. B. IgM^+ and IgM^- cells were sorted by FACS from SL and treated as above. For both A and B, the ROS of control group was set as 100%. Data are representatives of three independent experiments. *, $P < 0.05$; **, $P < 0.01$.

expressed widely on nearly all IgM^+ B cells and exerts different effects on the bacteria-uptake activity of PBL IgM^+ B cells and SL IgM^+ B cells. These results provide new insights into the endocytosis mechanism and activation regulation of B cells in teleost fish.

Acknowledgements

This work was supported by the grants from the National Natural Science Foundation of China (31528019), the AoShan Talents Program from Qingdao National Laboratory for Marine Science and Technology (No. 2015ASTP), and the Taishan Scholar Program of Shandong Province.

Appendix A. Supplementary data

Supplementary data to this article can be found online at https://doi.org/10.1016/j.fsi.2018.09.068.

References

[1] J. Li, D.R. Barreda, Y.A. Zhang, H. Boshra, A.E. Gelman, S. LaPatra, et al., B lymphocytes from early vertebrates have potent phagocytic and microbicidal abilities, Nat. Immunol. 7 (2006) 1116–1124.
[2] A. Rønneseth, H.I. Wergeland, E.F. Pettersen, Neutrophils and B-cells in atlantic cod (*Gadus morhua L.*), Fish Shellfish Immunol. 23 (2007) 493–503.
[3] H.S. Øverland, E.F. Pettersen, A. Rønneseth, H.I. Wergeland, Phagocytosis by B-cells and neutrophils in Atlantic salmon (*Salmo salar L.*) and Atlantic cod (*Gadus morhua L.*), Fish Shellfish Immunol. 28 (2010) 193–204.
[4] L.Y. Zhu, A.F. Lin, T. Shao, L. Nie, W.R. Dong, L.X. Xiang, et al., B cells in teleost fish act as pivotal initiating APCs in priming adaptive immunity: an evolutionary perspective on the origin of the B-1 cell subset and B7 molecules, J. Immunol. 192 (2014) 2699–2714.
[5] D.B. Ghebretnsae, H.I. Wergeland, G.T. Haugland, Functional characterization of IgM^+ B cells and adaptive immunity in lumpfish (*Cyclopterus lumpus L.*), Dev. Comp. Immunol. 52 (2015) 132–143.
[6] S. Yang, X. Tang, X. Sheng, J. Xing, W. Zhan, Development of monoclonal antibodies against IgM of half-smooth tongue sole (*Cynoglossus semilaevis*) and analysis of phagocytosis of fluorescence microspheres by $mIgM^+$ lymphocytes, Fish Shellfish Immunol. 66 (2017) 280–288.
[7] Y.Q. Li, L. Sun, J. Li, Internalization of large particles by turbot (*Scophthalmus maximus*) IgM^+ B cells mainly depends on macropinocytosis, Dev. Comp. Immunol. 82 (2018) 31–38.
[8] E.S. Edholm, E. Bengtén, J.L. Stafford, M. Sahoo, E.B. Taylor, N.W. Miller, et al., Identification of two IgD^+ B cell populations in channel catfish, *Ictalurus punctatus*, J. Immunol. 185 (2010) 4082–4094.
[9] J.D. Hansen, E.D. Landis, R.B. Phillips, Discovery of a unique Ig heavy-chain isotype (IgT) in rainbow trout: implications for a distinctive B cell developmental pathway in teleost fish, Proc. Natl. Acad. Sci. U.S.A. 102 (2005) 6919–6924.
[10] A.I. Ivanov, Pharmacological inhibition of endocytic pathways: is it specific enough to be useful? Meth. Mol. Biol. 440 (2008) 15–33.
[11] M. Ehrlich, W. Boll, A. Van Oijen, R. Hariharan, K. Chandran, M.L. Nibert, et al., Endocytosis by random initiation and stabilization of clathrin-coated pits, Cell 118 (2004) 591–605.
[12] J.P. Ferguson, S.D. Huber, N.M. Willy, E. Aygun, S. Goker, Mechanoregulation of clathrin-mediated endocytosis, J. Cell Sci. 130 (2017) 3631–3636.
[13] C. Commisso, S.M. Davidson, R.G. Soydaner-Azeloglu, S.J. Parker, J.J. Kamphorst, S. Hackett, et al., Macropinocytosis of protein is an amino acid supply route in Ras-transformed cells, Nature 497 (2013) 633–637.
[14] B.E. García-Pérez, J.J. De la Cruz-López, J.I. Castañeda-Sánchez, A.R. Muñóz-Duarte, A.D. Hernández-Pérez, H. Villegas-Castrejón, et al., Macropinocytosis is responsible for the uptake of pathogenic and non-pathogenic mycobacteria by B lymphocytes (Raji cells), BMC Microbiol. 12 (2012) 246–259.
[15] S. Wang, X. Huang, Y. Huang, X. Hao, H. Xu, M. Cai, et al., Entry of a novel marine DNA virus, Singapore grouper iridovirus, into host cells occurs via clathrin-mediated endocytosis and macropinocytosis in a pH-dependent manner, J. Virol. 88 (2014) 13047–13063.
[16] C.M. Grimaldi, R. Hicks, B. Diamond, B cell selection and susceptibility to autoimmunity, J. Immunol. 174 (2005) 1775–1781.
[17] Z. Keren, D. Melamed, Antigen receptor signaling competence and the determination of B cell fate in B-lymphopoiesis, Histol. Histopathol. 20 (2005) 187–196.
[18] E.A. Clark, CD22, a B cell-specific receptor, mediates adhesion and signal transduction, J. Immunol. 150 (1993) 4715–4718.
[19] K.L. Otipoby, K.B. Andersson, K.E. Draves, S.J. Klaus, A.G. Farr, J.D. Kerner, et al., CD22 regulates thymus-independent response and lifespan of B cells, Nature 384 (1996) 634–637.
[20] S. Sato, A.S. Miller, M. Inaoki, C.B. Bock, P.J. Jansen, M.L. Tang, et al., CD22 is both a positive and negative regulator of B lymphocyte antigen receptor signal transduction: altered signaling in CD22-deficient mice, Immunity 5 (1996) 551–562.
[21] Y.Q. Li, J. Zhang, J. Li, L. Sun, First characterization of fish CD22: an inhibitory role in the activation of peripheral blood leukocytes, Vet. Immunol. Immunopathol. 190 (2017) 39–44.
[22] H. Long, C. Chen, J. Zhang, L. Sun, Antibacterial and antiviral properties of tongue sole (*Cynoglossus semilaevis*) high mobility group B2 protein are largely independent on the acidic C-terminal domain, Fish Shellfish Immunol. 37 (2014) 66–74.
[23] Z.X. Zhou, L. Sun, Immune effects of R848: evidences that suggest an essential role of TLR7/8-induced, Myd88- and NF-κB-dependent signaling in the antiviral immunity of Japanese flounder (Paralichthys olivaceus), Dev. Comp. Immunol. 49 (2015) 113–120.
[24] B.C. Zhang, L. Sun, Tongue sole (*Cynoglossus semilaevis*) prothymosin alpha: cytokine-like activities associated with the intact protein and the C-terminal region that lead to anti-viral immunity via Myd88-dependent and -independent pathways respectively, Dev. Comp. Immunol. 53 (2015) 96–104.
[25] J.J. Wang, L. Sun, Edwardsiella tarda-regulated proteins in Japanese flounder (*Paralichthys olivaceus*): identification and evaluation of antibacterial potentials, J. Proteomics 124 (2015) 1–10.
[26] S. Malhotra, S. Kovats, W. Zhang, K.M. Coggeshall, B cell antigen receptor endocytosis and antigen presentation to T cells require Vav and dynamin, J. Biol. Chem. 284 (2009) 24088–24097.
[27] L. Vidard, M. Kovacsovics-Bankowski, S.K. Kraeft, L.B. Chen, B. Benacerraf, K.L. Rock, Analysis of MHC class II presentation of particulate antigens of B lymphocytes, J. Immunol. 156 (1996) 2809–2818.
[28] T. Tsubata, CD22 and CD72 are inhibitory receptors dominantly expressed in B lymphocytes and regulate systemic autoimmune diseases, Zeitschrift fur Rheumatologie 76 (2017) 10–13.
[29] S. Lumb, S.J. Fleischer, A. Wiedemann, C. Daridon, A. Maloney, A. Shock, et al., Engagement of CD22 on B cells with the monoclonal antibody epratuzumab stimulates the phosphorylation of upstream inhibitory signals of the B cell receptor, J. Cell Commun. Signal 10 (2016) 143–151.
[30] C.P. Chappell, K.E. Draves, E.A. Clark, CD22 is required for formation of memory B cell precursors within germinal centers, PLoS One 12 (2017) e0174661.
[31] J.C. Poe, T.F. Tedder, CD22 and Siglec-G in B cell function and tolerance, Trends Immunol. 33 (2012) 413–420.
[32] T.F. Tedder, J.C. Poe, K.M. Haas, CD22: a multifunctional receptor that regulates B lymphocyte survival and signal transduction, Adv. Immunol. 88 (2005) 1–50.
[33] L. Nitschke, R. Carsetti, B. Ocker, G. Köhler, M.C. Lamers, CD22 is a negative regulator of B-cell receptor signalling, Curr. Biol. 7 (1997) 133–143.